Roosting in exposed microsites by a nocturnal bird, the rufous-cheeked nightjar: implications for water balance under current and future climate conditions

Ryan S. O'Connor

DST-NRF Centre of Excellence at the Percy FitzPatrick Institute, Department of Zoology and Entomology, University of Pretoria, Private Bag X20, Hatfield 0028, South Africa.

Email: oconn163@gmail.com

R. Mark Brigham

Department of Biology, University of Regina, Regina, Saskatchewan S4S 0A2, Canada.

Email: Mark.Brigham@uregina.ca.

Andrew E. McKechnie*

DST-NRF Centre of Excellence at the Percy FitzPatrick Institute, Department of Zoology and Entomology, University of Pretoria, Private Bag X20, Hatfield 0028, South Africa.

South African Research Chair in Conservation Physiology, National Zoological Gardens of South Africa, P.O. Box 754, Pretoria 0001, South Africa.

Email: aemckechnie@zoology.up.ac.za.

* Author for correspondence

Abstract

Nocturnally active birds roosting in exposed diurnal microsites with intense solar radiation can experience operative temperatures (T_e) that markedly differ from air temperature (T_a). Quantifying T_e thus becomes important for accurately modeling energy and water balance. We measured T_e at roost and nest sites used by Rufous-cheeked Nightjars (*Caprimulgus rufigena*) with three-dimensionally printed biophysical models covered with the integument and plumage of a bird. Additionally, we estimated site-specific diurnal water requirements for evaporative cooling by integrating T_e and T_a profiles with evaporative water loss (EWL) data for Rufous-cheeked Nightjars. Between 12:00 and 15:00 hrs, average T_e at roost sites varied from 33.1 to 49.9 °C, whereas at the single nest site T_e averaged 51.4 °C. Average diurnal EWL, estimated using T_e, was as high as 10.5 and 11.3 g at roost and nest sites, respectively, estimates 3.8- and 4.0-fold greater, respectively, than when calculated with T_a profiles. These data illustrate that under current climatic conditions, Rufous-cheeked Nightjars can experience EWL potentially approaching their limits of dehydration tolerance. In the absence of microsite changes, climate change during the 21st century could perhaps create thermal conditions under which Rufous-cheeked Nightjars exceed dehydration tolerance limits before the onset of their nocturnal active phase.

Keywords: *Microclimate, evaporative cooling, biophysical ecology, operative temperature, Caprimulgus rufigena, Rufous-cheeked Nightjar*

Introduction

Organisms frequently experience the thermal environment at fine spatial scales, typically relative to their body size, resulting in microclimates that substantially differ from coarse regional macroclimates derived from standardized weather data (Beckman et al. 1973, Campbell and Norman 1998, Potter et al. 2013). An organisms immediate thermal environment arises from a complex suite of interacting abiotic variables, including solar and thermal radiation, air temperature (T_a), wind speed, surface temperature and humidity (Porter and Gates 1969, Bakken 1976, Bakken 1989). Due to the fine scale at which microclimates occur, animals occupying the same habitat can simultaneously experience a thermally diverse range of microclimates (Sears et al. 2011), leading to large variation among individuals in energy and water demands. Behaviorally, animals may control their rate of heat loss or gain through postural changes (Porter et al. 1994) and/or by occupying thermally-buffered refugia (Wolf et al. 1996, Scheffers et al. 2014). Additionally, endotherms may temporarily abandon normothermic T_b by expressing patterns of thermoregulation that lead to energy and water conservation (e.g., facultative hypothermia or hyperthermia; McKechnie and Lovegrove 2002, Tieleman and Williams 1999), conditions under which microhabitat selection will have a large influence on energy and/or water savings. A thorough understanding of the microclimates an individual experiences within its habitat is thus a prerequisite for predicting energy and water requirements under current and future climates (Kearney and Porter 2009, Porter et al. 2010).

Operative temperature (T_e), the temperature of an animal model in thermodynamic equilibrium with its environment in the absence of metabolic heating or evaporative cooling (Bakken 1976), is commonly used to quantify microclimates at spatial scales relevant to an animal (Bakken 1992, Dzialowski 2005). Operative temperature can be measured using either

63 mathematical, statistical or biophysical models (Bakken 1992, Angilletta 2009). Biophysical
64 models traditionally consist of a thin copper cast electroformed to match the size and shape of
65 the focal animal and, in the case of ectotherms that lack pelages, painted to match the
66 absorptivity of the focal species (Bakken and Gates 1975, Dzialowski 2005). For thermal
67 investigations of endotherms, the skin and pelage of the animal of interest is typically wrapped
68 around the cast to incorporate the thermal properties of fur or feathers (e.g., Ward and Pinshow
69 1995, Bozinovic et al. 2000, Tieleman and Williams 2002). Hence, biophysical models integrate
70 the abiotic factors of the thermal environmental (i.e., radiation, T_a, wind speed and surface
71 temperature) with an animal's physical attributes (i.e., size, shape and color) to determine the T_e
72 experienced in a particular microsite (Bakken and Angilletta 2014).
73 Nightjars and nighthawks (Caprimulgidae) are a nocturnally active avian taxon that
74 generally roost and nest on the ground during their diurnal rest phase. Several species have been
75 reported occupying sites devoid of shade and continuously subjected to intense solar radiation,
76 even in midsummer (e.g., Cowles and Dawson 1951, Bartholomew et al. 1962, Steyn 1971,
77 Grant 1982, Cleere and Nurney 1998). Moreover, forced convective heat loss at these sites is
78 likely minimal due to reduced wind speeds at ground level (Chen et al. 1998). Caprimulgids,
79 therefore, can experience microclimates wherein T_e peaks at 50 - 60 ºC (Weller 1958, Grant
80 1982, Ingels et al. 1984). Under such extreme heat, caprimulgids must elevate evaporative water
81 loss (EWL) above baseline levels for prolonged periods to avoid lethal hyperthermia (Grant
82 1982, O'Connor et al. 2017b).
83 Our objectives were to characterize the microclimates of roost and nest sites for a
84 southern African arid-zone caprimulgid, the Rufous-cheeked Nightjar (*Caprimulgus rufigena*).
85 Like many other nightjars, Rufous-cheeked Nightjars may select roost and/or nest sites with

partial or no shading, even in mid-summer (R.S. O'Connor personal observation, Cleere and Nurney 1998). No attempts, however, have been made to quantify the range of T_e values that Rufous-cheeked Nightjars experience in the field, despite the importance of these data for understanding their water budgets. We used two types of three dimensionally (3-D) printed biophysical models to measure T_e at roost and nest sites, one consisting of a 3-D printed plastic body (hereafter $T_{e\text{-plastic}}$) and the second type a plastic body covered with the skin and feathers of a Rufous-cheeked Nightjar (hereafter $T_{e\text{-skin}}$). We also integrated T_e and T_a profiles measured at each site with EWL data derived from a laboratory heat tolerance investigation for this species (O'Connor et al. 2017b) to predict site-specific water requirements for evaporative cooling during the diurnal inactive period.

Methods

Roost and nest location

We quantified T_e at six roost sites and one nest site used by six Rufous-cheeked Nightjars (two roost sites were used by the same individual) between 26 October and 12 December 2015 at Dronfield Nature Reserve (28º 39' S, 24º 48' E, ~1218 m a.s.l.) near Kimberley, South Africa. Nightjars were captured at night on roads with a handheld net and spotlight. Upon capture, we fitted nightjars with a radio transmitter (BD-2T, Holohil Systems, Carp, Ontario, Canada) positioned between the scapulars using a backpack-style harness built from Teflon ribbon (Telonics, Mesa, AZ, USA). Additionally, we injected a passive-integrated transponder (PIT) tag (Biomark, Boise, ID, USA) into the peritoneal cavity to register T_b of incubating adults as part of a separate thermoregulation study (O'Connor et al. 2017a). Birds were released immediately after transmitters were attached and PIT tags injected. We tracked birds to their roost sites using

telemetry. Once a site was located, we recorded the latitude and longitude and marked the location with a metal stake for eventual placement of our models. On average, models were set up 3.5 days after discovering a roost location. For the nest site, we waited until incubation was complete before placing our models.

Biophysical model construction and T_e measurements

We followed Watson and Francis (2015) and used 3-D printed models to measure T_e. These authors compared T_e values of 3-D printed models to those recorded using traditional electroformed copper models and found that T_e distributions of the two model types were generally similar when placed in identical habitats. Furthermore, Watson and Francis (2015) reported no substantial differences in the response of models to radiant heat or varying T_a. Finally, 3-D printed models are more anatomically accurate and easier to produce than traditional electroformed copper models, and hence are a good substitute for measuring T_e (Watson and Francis 2015).

We constructed four 3-D printed biophysical models, consisting of two $T_{e\text{-skin}}$ models and two $T_{e\text{-plastic}}$ models. To construct our $T_{e\text{-plastic}}$ models, we took a series of 49 pictures at 90º and 45º angles encompassing 360º of a deceased Rufous-cheeked Nightjar (Supplementary Material A, Figure S1). These photos were uploaded to 123d Catch (http://www.123dapp.com/catch) which automatically stitched them into a 3-D model. Because we were unable to capture photos of the bird's ventral surface during this procedure, we used Blender v. 2.75 (https://www.blender.org/) to manually impose a plane to the underside of each model. The digital 3-D model was then scaled using Cura (https://ultimaker.com/en/products/cura-software) and saved as an .stl file and emailed to 3DForms (Johannesburg, South Africa,

http://www.3dforms.co.za/) for printing. The $T_{e\text{-}plastic}$ models were printed using Makerbot's (Makerbot Industries LLC, Brooklyn, NY, USA) cool grey acrylonitrile butadiene styrene (ABS) filament with a 0% fill and an approximately 2-mm thick shell. The final $T_{e\text{-}plastic}$ models were smoothed post printing, and measured approximately 225 mm from tip of bill to tail, 44 mm from top of head to base and 53 mm wide. The $T_{e\text{-}plastic}$ models were printed with a removable lid on the base, which we secured with adhesive prior to model deployment (Supplementary Material A, Figure S2). A type-T thermocouple (Omega, Norwalk, CT, USA) was inserted through a hole drilled in the base of each model and sealed in place with an adhesive. The tip of the thermocouple was centered horizontally and vertically within the model to avoid any effects of thermal stratification (Bakken 1992; Supplementary Material A, Figure S2). Prior to deployment, thermocouples were calibrated in a water bath between 5 and 50 ºC in 5 ºC increments against a mercury thermometer traceable to the US National Bureau of Standards.

To construct our $T_{e\text{-}skin}$ models, we provided two Rufous-cheeked Nightjar carcasses to a taxidermist who separated the skin from the bodies. We took 32 pictures in series of a skinned body, again encompassing 360º and taken at 90º and 45º angles (Supplementary Material A, Figure S3). These photos were compiled, scaled and printed using the same software and plastic as outlined above. We scaled these models based on measurements provided by the taxidermist, with the final dimensions of the body measuring approximately 39.5 mm long x 14 mm wide x 23.4 mm high. Due to the smaller size of these models, they had to be printed in halves and then glued together. Consequently, some tiny gaps remained on the models and we sealed these using plaster-of-Paris and a cyanoacrylate adhesive (Supplementary Material A, Figure S4). We ensured models were airtight by completely submerging them in water to observe if any escaping air bubbles formed. We inserted a type-T thermocouple (Omega, Norwalk, CT, USA) into the

approximate center of each model through a hole drilled in the ventral surface. Thermocouples were sealed in place and calibrated prior to placement as described for the $T_{e\text{-}plastic}$ models above. The final plastic bodies were then returned to the taxidermist who wrapped them in the skin to create the complete $T_{e\text{-}skin}$ models. Because the smoothing process left the 3-D printed plastic bodies slippery, the taxidermist had to wrap a ~5-mm layer of cotton wool around the bodies to increase adhesion between the skin and the plastic (Supplementary Material A, Figure S5).

Both $T_{e\text{-}skin}$ and $T_{e\text{-}plastic}$ models were placed side by side at a specific site (Supplementary Material A, Figure S6) either in the morning (mean placement time = 07:48) or at night (mean placement time = 19:12). Models were first placed facing true north, whereafter we alternated the cardinal direction approximately every 24 hours (mean time in each direction = 22.9 hours), with the models positioned in every cardinal direction before relocation to a new site. Therefore, the mean time models remained at a site was approximately 4 days (mean time at a site = 3.8 days). We recorded $T_{e\text{-}skin}$ and $T_{e\text{-}plastic}$ values simultaneously every minute using a 4-channel thermocouple data logger (model SD-947, Reed Instruments, Wilmington, NC, USA). We buried the thermocouple wiring between the models and logger in the sand to prevent heat from solar radiation conducting along the wire (Bakken 1992). Operative temperature data were transferred onto a personal computer every time we changed the direction of the models. Weather data were recorded every minute with a portable weather station (Vantage Pro2, Davis Instruments, Hayward, CA, USA), placed ~2.0 m above the ground and calibrated as described by Smit et al. (2013).

Data analysis

All analyses were conducted in R v. 3.4.0 (R Core Team 2017) with values presented as mean ± standard deviation (SD). We categorized the data into three periods, namely diurnal (i.e., sunrise to sunset), midday (i.e., 12:00 – 15:00 hours) and nocturnal (i.e., sunset to sunrise). Sunrise and sunset times were calculated using the R package *maptools* (Bivand and Lewin-Koh 2017). We compared overall differences among $T_{e\text{-}skin}$ and $T_{e\text{-}plastic}$ models for all sites combined during the diurnal period by fitting a linear mixed-effect model using the R package *lme4* (Bates et al. 2015), with T_e a continuous response variable and *skin* a two-level categorical predictor. We included T_e model as a random factor because of repeated T_e measurements within the same model. We report the effect size *skin* had on T_e, represented as the parameter estimate ($\beta \pm$ SD) and the associated 95% confidence interval (95% CI). We considered the mean difference between $T_{e\text{-}skin}$ and $T_{e\text{-}plastic}$ models to be statistically significant if the 95% CI did not overlap zero. We then analyzed diel patterns in $T_{e\text{-}skin}$ and T_a at each site by aggregating all values recorded each minute during a recording period and taking the average. For example, mean $T_{e\text{-}skin}$ at 12:00 hours within a site represents the average of all $T_{e\text{-}skin}$ values recorded at 12:00 hours at that site over the entire recording period. Because there were occasional gaps in our temperature recordings (e.g., when changing position of the models), not every minute was represented for every day and consequently sample sizes for each minute ranged from 1 to 5. To determine when and for how long $T_{e\text{-}skin}$ exceeded free-ranging modal body temperature ($T_{b\text{-}mod}$), we isolated all diurnal T_e values > 39.7 ºC at roost sites and all T_e values > 38.8 ºC at the nest site (O'Connor et al. 2017a). We additionally calculated the direction and magnitude that $T_{e\text{-}skin}$ deviated from free-ranging $T_{b\text{-}mod}$ at each site during the diurnal and midday periods by subtracting $T_{b\text{-}mod}$ from each $T_{e\text{-}skin}$ value (i.e., $\Delta T_e - T_{b\text{-}mod}$). Overall roost site averages represent the combined average from each individual roost site average.

To estimate site-specific diurnal EWL during a recording period, we integrated T_e and T_a traces with the EWL data reported by O'Connor et al. (2017b). We used free-ranging $T_{b\text{-}mod}$ for roosting birds (i.e., 39.7 ºC; O'Connor et al. 2017a) as an inflection point at roost sites and the $T_{b\text{-}mod}$ of an incubating Rufous-cheeked Nightjar (i.e., 38.8 ºC; O'Connor et al. 2017a) as an inflection point at the nest site. At T_a and $T_e \leq T_{b\text{-}mod}$, we predicted EWL assuming EWL (g hr^{-1}) = $0.007x + 0.002$, and at T_a and $T_e > T_{b\text{-}mod}$ we assumed EWL (g hr^{-1}) = $0.099x - 3.610$, where x represents either T_e or T_a. For all T_e calculations we used $T_{e\text{-}skin}$ values. We calculated a mean EWL estimate for each minute over a 24-hour period by aggregating all values at each minute as described above for the diel $T_{e\text{-}skin}$ and T_a calculations. We then summed all mean EWL predictions for each minute between sunrise and sunset to obtain the total average amount of water lost during just the diurnal period at a given site. We expressed total EWL during the diurnal period as a percentage of body mass (M_b) assuming an average M_b of 57.1 g, which was the average M_b of birds at capture when being weighed for a total body water study (O'Connor et al. *unpublished data*).

Results

We recorded 36,648 T_e values for each model type. Except for a single roost situated under a camelthorn (*Vachellia erioloba*) tree, and thus shaded for most of the day, all roost sites were partially shaded and experienced periods of full solar exposure throughout the day. In contrast, the nest site was completely exposed and hence continuously subjected to intense solar radiation. Average diurnal T_a across sites during the study period was 28.0 ± 2.8 ºC and average solar radiation level was 544.5 ± 37.3 W m^{-2}. Within each site, mean $T_{e\text{-}skin}$ values were generally similar to those of $T_{e\text{-}plastic}$ during both the diurnal and midday periods (Table 1). On average,

mean $T_{e\text{-}plastic}$ values were 0.9 ± 2.0 ºC greater than $T_{e\text{-}skin}$ values during the diurnal period and 0.2 ± 0.6 ºC greater during the midday period (Table 1). In contrast, differences between mean maximum T_e within sites were larger (Table 1), with mean maximum $T_{e\text{-}plastic}$ values 3.4 ± 3.7 ºC greater than mean $T_{e\text{-}skin}$ values. The overall difference between $T_{e\text{-}skin}$ and $T_{e\text{-}plastic}$ models during the diurnal period for all sites combined was not significant (skin β = -0.920 ± 3.48 ºC, 95% CI = -8.14 ºC, 5.93 ºC), with mean $T_{e\text{-}skin}$ = 36.3 ± 10.8 ºC and mean $T_{e\text{-}plastic}$ = 37.3 ± 11.5 ºC.

During the nocturnal period, T_e did not deviate far from T_a at roost sites or the nest site (Figure 2 and Figure 3). For example, the mean difference between $T_{e\text{-}skin}$ and T_a during the nocturnal period at roost and nest sites combined was 0.6 ± 2.3 ºC (range = -6.8 – 8.8 ºC). Beginning at sunrise, however, T_e increased rapidly to values far above T_a (Figure 2 and Figure 3). Except for at roosts 3 and 5, mean $T_{e\text{-}skin}$ exceeded free-ranging $T_{b\text{-}mod}$ for extended periods (Figure 2). On average, $T_{e\text{-}skin}$ from roost sites exceeded $T_{b\text{-}mod}$ by 08:27 h (range = 08:12 – 08:41 h; Figure 2). The overall average duration that $T_{e\text{-}skin}$ exceeded $T_{b\text{-}mod}$ during the diurnal period at roost sites was 6.8 hours (range = 4.6 – 7.9 hours; Figure 2). During this time, overall mean $T_{e\text{-}skin}$ = 43.6 ± 3.5 ºC (range = 39.9 – 48.9 ºC) while the overall average T_a = 33.2 ± 3.5 ºC (range = 28.1 – 38.0 ºC). During the midday period, mean $\Delta T_e - T_{b\text{-}mod}$ among roost sites ranged from – 6.6 ± 3.3 to 10.2 ± 7.6 ºC (Figure 4).

Mean total diurnal EWL estimated based on $T_{e\text{-}skin}$ ranged from 2.8 – 10.5 g among roost sites, with evaporative water requirements being 1.2 – 3.8-fold greater when calculated using T_e compared with estimates based on T_a (Figure 5). Expressed as a percentage of M_b, total diurnal EWL among roost sites ranged from 4.9 – 18.4% of M_b.

At the nest site, mean $T_{e\text{-}skin}$ exceeded incubating $T_{b\text{-}mod}$ by 09:33 and did not decrease below $T_{b\text{-}mod}$ until 18:20 (~8.75 hours; Figure 3). During this period, $T_{e\text{-}skin}$ averaged 48.0 ± 4.0

246 ºC (range = 38.9 – 53.4 ºC), while average T_a = 31.3 ± 1.7 ºC (range = 26.6 – 33.5 ºC). The
247 average $\Delta T_e - T_{b\text{-}mod}$ during the midday period at the nest site was 12.6 ± 4.2 ºC (Figure 4).
248 Diurnal evaporative water requirements at the nest site were 11.3 g when estimated from $T_{e\text{-}skin}$, a
249 value 4-fold greater than when estimated using T_a values (Figure 6). Total estimated diurnal
250 water loss at the nest site was equivalent to 19.8% of M_b.
251
252 **Discussion**
253 We show that Rufous-cheeked Nightjars regularly experienced microclimates where T_e
254 substantially exceeded free-ranging T_b (O'Connor et al 2017a). The high environmental
255 temperatures reported here are consistent with those reported by previous authors who
256 characterized the diurnal thermal environments occupied by nightjars and other thermally
257 exposed birds (e.g., Weller 1958, Bartholomew and Dawson 1979, Grant 1982, Tieleman and
258 Williams 2002, Amat and Masero 2004a, Carroll et al. 2015a). Our data further underscore the
259 significant contribution that solar radiation can have on the total heat load of an animal and that
260 T_a alone typically provides only a minimum index of a terrestrial animal's thermal stress in hot
261 environments (Porter and Gates 1969, Sears et al. 2011). This is exemplified by the fact that
262 maximum T_a exceeded 38 ºC on just 3 days during our recording period whereas maximum T_e
263 exceeded 38 ºC on 27 days.
264 We did not find significant differences in average diurnal T_e measurements among our $T_{e\text{-}$
265 $skin}$ and $T_{e\text{-}plastic}$ models. In a similar study, Walsberg and Weathers (1986) compared T_e values
266 from copper taxidermic mounts covered with the integument of four bird species to T_e values
267 recorded from painted metal spheres. When averaged over a 5-day period, Walsberg and
268 Weathers (1986) found that mean differences among the models were less than 2.0 ºC. However,

Walsberg and Weathers (1986) noted that when T_e was averaged over time scales of less than several hours, differences between models reached up to 6.3 ºC. Indeed, this likely explains the larger differences we observed among our models for mean maximum T_e because these averages were derived from single point estimates as opposed to data spanning more than several hours. Hence, our findings support the conclusion reached by Walsberg and Weathers (1986) that complex T_e models may not always be necessary, as long as numerous data are collected over extended periods. Likewise, Bakken (1992) suggested that in some instances, a rough approximate representation of the study animal can be adequate and the appropriate T_e model used will depend on the relative importance of several considerations, such as field conditions or the study's objective. However, investigators should attempt to use models with physical properties matching those of a study animal whenever possible (Bakken 1992, Bakken and Angilletta 2014).

Our data show that predicted diurnal water requirements can be several-fold greater when calculated using T_e compared to T_a, reiterating the importance of using spatially relevant microclimates when assessing an animal's physiological stress (Huey 1991, Helmuth et al. 2010, Porter et al. 2010). Moreover, the amount of water lost based on T_e values was equivalent to a substantial percentage of M_b, suggesting that, on hot, cloudless days, Rufous-cheeked Nightjars might be approaching their limits of dehydration tolerance. Unfortunately, few data exist on acute dehydration tolerance among birds when exposed to severe heat stress over time scales of hours on very hot days (Wolf 2000, McKechnie and Wolf 2010, Albright et al. 2017). Wolf and Walsberg (1996), however, reported acute dehydration tolerance limits in Verdins (*Auriparus flaviceps*; ~7 g) when water loss exceeded 11% of M_b, a physiological threshold far lower than the maximum water losses predicted here. An important factor known to enhance dehydration

292 tolerance among birds and mammals is the ability to conserve plasma volume (Horowitz and
293 Borut 1970, Arad et al. 1989, Carmi et al. 1993). However, plasma volume conservation is
294 apparently affected by the T_a at which dehydration occurs (Carmi et al. 1994). Carmi et al.
295 (1994), for example, found that Rock Pigeons (*Columbia livia*) could maintain plasma volume at
296 T_a of 36 °C for ~32 hours but, when exposed to T_a of 40 °C for ~28 hours, plasma volume
297 decreased by 8.9%, despite similar total losses in water between the T_a groups. To our
298 knowledge, there are no data on whether caprimulgids conserve plasma volume during acute heat
299 stress, but we speculate that Rufous-cheeked Nightjars and relatives have evolved mechanisms
300 increasing permeability for osmotic diffusion between the extracellular and intracellular
301 compartments, thereby aiding plasma volume conservation and allowing them to tolerate
302 prolonged periods of high EWL.

303 Despite a large rapid depletion of body water during the diurnal rest phase, we predict that
304 Rufous-cheeked Nightjars with a mean M_b of 57.1 g can periodically replenish body water by
305 obtaining a maximum of 10.3 g H_2O through preformed and metabolic water (Supplementary
306 Material B). However, the temporal window for nightjars to forage is highly variable and
307 constrained by several ecological and environmental factors (Mills 1986, Jetz et al. 2003,
308 Ashdown and McKechnie 2008, Woods and Brigham 2008). Consequently, nightjars may not
309 always acquire enough insects to offset EWL, increasing their dependence on drinking water.
310 Indeed, on multiple occasions at dusk we observed Rufous-cheeked Nightjars drinking on the
311 wing at water reservoirs near roost and nest sites. Furthermore, assuming a proportional increase
312 in T_e with the projected 4 °C increase in T_a during the 21st century (Smith et al. 2011), maximum
313 predicted water requirements at roost and nest sites for Rufous-cheeked Nightjars at Dronfield
314 could reach values of 13.8 and 15.1 g, respectively, equivalent to 24.2 and 26.4% of M_b.

315 Presumably, nightjar populations with no access to drinking water will be highly vulnerable to
316 climate change because of the increasing difficulty of offsetting water deficits solely through
317 preformed and metabolic water.

318 Given the design and construction of our T_e models, it is possible that multiple sources of
319 error were introduced in our T_e estimates. Firstly, the size difference between our 3-D printed
320 bodies could have created issues with thermal stratification (Bakken 1992, O'Connor et al. 2000,
321 Bakken and Angilletta 2014). However, the generally small size of our models (< 100 g)
322 combined with the thickness of the plastic (~2 mm) and the placement of the thermocouples
323 likely mitigated this issue (Bakken 1992). The second potential source of error stems from the
324 layer of cotton wool wrapped around the plastic body of our $T_{e\text{-}skin}$ models. This cotton added an
325 insulative layer which likely increased the time constant of our models. Bakken (1992) and
326 O'Connor (2000) proposed that the time constant desired ultimately depends on the study
327 question and rapid time responses are plausibly more important in studies on animals where
328 behavioral thermoregulation is paramount (e.g., ectotherms). Because nightjars are inactive
329 during the day, behavioral thermoregulation is minimal, aside from postural adjustments, and an
330 instantaneous time constant may not be as imperative. In any event, because we lacked the
331 necessary equipment (e.g., wind tunnel and solar simulator), we could not accurately calibrate
332 our models prior to use, an issue that appears to be common among operative temperature studies
333 (Walsberg and Wolf 1996, Dzialowski 2005).
334

335 **Conclusions**

336 One of the most pressing issues facing biologists today is predicting how organisms will respond
337 to climate change (Schwenk et al. 2009, Sears and Angilletta 2011). A vital step towards

338 addressing this issue is knowing the degree to which an organism is exposed to environmental
339 change (Williams et al. 2008). Organismal exposure, however, will be mediated through
340 microhabitat selection and the use of microrefugia which can substantially buffer or amplify an
341 environmental signal (e.g., Woods et al. 2015, Morelli et al. 2016, Pincebourde et al. 2016,
342 Lenoir et al. 2017). Hence, organisms usually experience microclimates at spatial scales much
343 finer than those recorded at gridded weather stations (Campbell and Norman 1998, Helmuth et
344 al. 2010). An understanding of the thermal heterogeneity an organism is exposed to across its
345 range of microclimates is necessary when assessing its physiological stress under current and
346 future climate conditions.

347 During our study, Rufous-cheeked Nightjars experienced microclimates where T_e
348 substantially exceeded normothermic T_b for periods of several hours each day. Although
349 diurnally active birds may also experience similarly high environmental temperatures when
350 foraging, they also can periodically escape midday heat by seeking out shaded microhabitats
351 with more moderate microclimates (Goldstein 1984, Carroll et al. 2015b, Pattinson and Smit
352 2017). Hence, diurnal birds can reduce rates of EWL through behavioral thermoregulation
353 (Williams et al. 1999, Wolf 2000). In contrast, nightjars remain inactive and experience the full
354 brunt of the sun, resulting in large evaporative water requirements (Grant 1982). The capacity for
355 nightjars to tolerate high heat loads stems from a combination of a low resting metabolic rate and
356 an energetically efficient mechanism for dissipating heat (Dawson and Fisher 1969, O'Connor et
357 al. 2017b, Talbot et al. 2017). Both of these traits serve to reduce an individual's total heat load
358 by minimizing endogenous heat production. Several authors have suggested that the use of
359 exposed sites by ground nesting species presents a trade-off between lower predation risk due to
360 early predator detection and increased heat stress (Amat and Masero 2004b, Tieleman et al.

2008). However, increasing temperatures could alter the dynamics of this trade-off, possibly forcing nightjars to use more shaded microhabitats despite greater predation risk. Our EWL estimates based on T_e values suggest that Rufous-cheeked Nightjars require exceedingly high EWL rates. The physiological mechanisms allowing nightjars to tolerate large losses in body water are presently unknown, but could pertain to an increased capacity to maintain plasma volume. Additionally, free-ranging Rufous-cheeked Nightjars likely conserve water through facultative hyperthermia (O'Connor et al. 2017a). Under current thermal conditions, Rufous-cheeked Nightjars can apparently offset evaporative water losses with preformed water from their diet and metabolic water. Climate change, however, will likely increase evaporative water requirements, in turn increasing the importance of drinking water and, possibly, even resulting in conditions where nightjars cannot make it to sunset without becoming lethally dehydrated.

Acknowledgements

We sincerely thank Alex Mullinos at 3dforms for his patience and help with 3-D printing and Dr. James Meyer for performing the taxidermy necessary to complete the models. Without their assistance, this study would not have been possible. We additionally thank Duncan MacFadyen and E. Oppenheimer & Son for granting us access to their property. Cathy Bester and all field assistants provided invaluable help during the field season. Lastly, Bruce Woodroffe and Awesome Tools (Cape Town, South Africa) provided discounted lighting equipment, for which we are greatly appreciative.

References

Albright, T.P., Mutiibwa, D., Gerson, A.R., Smith, E.K., Talbot, W.A., O'Neill, J.J., McKechnie, A.E., and Wolf, B.O. 2017. Mapping evaporative water loss in desert passerines reveals an expanding threat of lethal dehydration. Proc. Natl. Acad. Sci. **114**(9): 2283–2288. doi:10.1073/pnas.1613625114.

Amat, J.A., and Masero, J.A. 2004a. How Kentish plovers, *Charadrius alexandrinus*, cope with heat stress during incubation. Behav. Ecol. Sociobiol. **56**(1): 26–33. doi:10.1007/s00265-004-0758-9.

Amat, J.A., and Masero, J.A. 2004b. Predation risk on incubating adults constrains the choice of thermally favourable nest sites in a plover. Anim. Behav. **67**(2): 293–300. doi:10.1016/j.anbehav.2003.06.014.

Arad, Z., Horowitz, M., Eylath, U., and Marder, J. 1989. Osmoregulation and body fluid compartmentalization in dehydrated heat-exposed pigeons. Am. J. Physiol. **257**: R377-R382.

Ashdown, R.A.M., and McKechnie, A.E. 2008. Environmental correlates of freckled nightjar (*Caprimulgus tristigma*) activity in a seasonal, subtropical habitat. J. Ornithol. **149**(4): 615–619. doi:10.1007/s10336-008-0309-7.

Bakken, G.S. 1976. A heat transfer analysis of animals: unifying concepts and the application of metabolism chamber data to field ecology. J. Therm. Biol. **60**: 337–384.

Bakken, G.S. 1989. Arboreal perch properties and the operative temperature experienced by small animals. Ecology **70**(4): 922–930.

Bakken, G.S. 1992. Measurement and application of operative and standard operative temperatures in ecology. Am. Zool. **32**(2): 194–216. doi:10.1093/icb/32.2.194.

404 Bakken, G.S., and Angilletta, M.J. 2014. How to avoid errors when quantifying thermal
405 environments. Funct. Ecol. **28**(1): 96–107. doi:10.1111/1365-2435.12149.
406 Bartholomew, G.A., and Dawson, W.R. 1979. Thermoregulatory behavior during incubation in
407 Heermann's gulls. Physiol. Zool. **52**(4): 422–437.
408 Bartholomew, G.A., Hudson, J.W., and Howell, T.R. 1962. Body temperature, oxygen
409 consumption, evaporative water loss, and heart rate in the poor-will. Condor **64**: 117–125.
410 Bates, D., Mächler, M., Bolker, B., and Walker, S. 2015. Fitting linear mixed-effects models
411 using lme4. J. Stat. Softw. **67**(1): 1–48. doi:10.18637/jss.v067.i01.
412 Beckman, W.A., Mitchell, J.W., and Porter, W.P. 1973. Thermal model for prediction of a desert
413 iguana's daily and seasonal behavior. J. Heat Transfer **95**(2): 257. doi:10.1115/1.3450037.
414 Bivand, R., and Lewin-Koh, N. 2017. maptools: tools for reading and handling spatial objects. R
415 Package Version 0.9-2. https://CRAN.R-project.org/package=maptools.
416 Bozinovic, F., Lagos, J.A., Vásquez, R.A., and Kenagy, G. 2000. Time and energy use under
417 thermoregulatory constraints in a diurnal rodent. J. Therm. Biol. **25**(3): 251–256.
418 doi:10.1016/S0306-4565(99)00031-5.
419 Carmi, N., Pinshow, B., and Horowitz, M. 1994. Plasma volume conservation in pigeons: effects
420 of air temperature during dehydration. Am. J. Physiol. **267**: R1449–R1453.
421 Carmi, N., Pinshow, B., Horowitz, M., and Bernstein, M.H. 1993. Birds conserve plasma volume
422 during thermal and flight-incurred dehydration. Physiol. Zool. **66**(5): 829–846.
423 Carroll, J.M., Davis, C.A., Elmore, R.D., and Fuhlendorf, S.D. 2015a. A ground-nesting
424 galliform's response to thermal heterogeneity: implications for ground-dwelling birds. PLoS
425 One **10**(11): e0143676. doi:10.1371/journal.pone.0143676.
426 Carroll, J.M., Davis, C.A., Elmore, R.D., Fuhlendorf, S.D., and Thacker, E.T. 2015b. Thermal

patterns constrain diurnal behavior of a ground-dwelling bird. Ecosphere **6**(11): art222. doi:10.1890/ES15-00163.1.

Chen, Y.C., Bundy, D.S., and Hoff, S.J. 1998. Modeling the variation of wind speed with height for agricultural source pollution control. Agric. Biosyst. Eng. Publ. **104**(1B): 1685–1691.

Cowles, R.B., and Dawson, W.R. 1951. A cooling mechanism of the Texas nighthawk. Condor **53**(1): 19–22.

Dawson, W.R., and Fisher, C.D. 1969. Responses to temperature by the spotted nightjar (*Eurostopodus guttatus*). Condor **71**(1): 49–53.

Dzialowski, E.M. 2005. Use of operative temperature and standard operative temperature models in thermal biology. J. Therm. Biol. **30**(4): 317–334. doi:10.1016/j.jtherbio.2005.01.005.

Goldstein, D.L. 1984. The thermal environment and its constraint on activity of desert quail in summer. Auk **101**(July): 542–550.

Grant, G.S. 1982. Avian incubation: egg temperature, nest humidity, and behavioral thermoregulation in a hot environment. Ornithol. Monogr. **30**(30): iii-75. doi:10.2307/40166669.

Helmuth, B., Broitman, B.R., Yamane, L., Gilman, S.E., Mach, K., Mislan, K.A.S., and Denny, M.W. 2010. Organismal climatology: analyzing environmental variability at scales relevant to physiological stress. J. Exp. Biol. **213**(6): 995–1003. doi:10.1242/jeb.038463.

Horowitz, M., and Borut, A. 1970. Effect of acute dehydration on body fluid compartments in three rodent species, *Rattus norvegicus*, *Acomys cahirinus* and *Meriones crassus*. Comp. Biochem. Physiol. **35**: 283–290.

Huey, R.B. 1991. Physiological consequences of habitat selection. Am. Nat. **137**: S91–S115. doi:10.1086/285141.

450 Ingels, J., Ribot, J.H., and de Jong, B.H.J. 1984. Vulnerability of eggs and young of the blackish
451 nightjar (*Caprimulgus nigrescens*) in Suriname. Auk **101**(2): 388–391.
452 Jetz, W., Steffen, J., and Linsenmair, K. 2003. Effects of light and prey availability on nocturnal,
453 lunar and seasonal activity of tropical nightjars. Oikos **103**(3): 627–639.
454 doi:10.1034/j.1600-0706.2003.12856.x.
455 Kearney, M., and Porter, W. 2009. Mechanistic niche modelling: combining physiological and
456 spatial data to predict species' ranges. Ecol. Lett. **12**(4): 334–350. doi:10.1111/j.1461-
457 0248.2008.01277.x.
458 Lenoir, J., Hattab, T., and Pierre, G. 2017. Climatic microrefugia under anthropogenic climate
459 change: implications for species redistribution. Ecography. **40**(2): 253–266.
460 doi:10.1111/ecog.02788.
461 McKechnie, A.E., and Lovegrove, B.G. 2002. Avian facultative hypothermic responses: a
462 review. Condor **104**: 705–724. doi:10.1650/0010-5422.
463 McKechnie, A.E., and Wolf, B.O. 2010. Climate change increases the likelihood of catastrophic
464 avian mortality events during extreme heat waves. Biol. Lett. **6**(2): 253–6.
465 doi:10.1098/rsbl.2009.0702.
466 Mills, A.M. 1986. The influence of moonlight on the behavior of goatsuckers (Caprimulgidae).
467 Auk **103**(2): 370–378.
468 Morelli, T.L., Daly, C., Dobrowski, S.Z., Dulen, D.M., Ebersole, J.L., Jackson, S.T., Lundquist,
469 J.D., Millar, C.I., Maher, S.P., Monahan, W.B., Nydick, K.R., Redmond, K.T., Sawyer,
470 S.C., Stock, S., and Beissinger, S.R. 2016. Managing climate change refugia for climate
471 adaptation. PLoS One **11**(8): e0159909. doi:10.1371/journal.pone.0159909.
472 O'Connor, M.P., Zimmerman, L.C., Dzialowski, E.M., and Spotila, J.R. 2000. Thick-walled

physical models improve estimates of operative temperatures for moderate to large-sized reptiles. J. Therm. Biol. **25**(4): 293–304. doi:10.1016/S0306-4565(99)00101-1.

O'Connor, R.S., Brigham, R.M., and McKechnie, A.E. 2017a. Diurnal body temperature patterns in free-ranging populations of two southern African arid-zone nightjars. J. Avian Biol. **48**(9): 1195–1204. doi:10.1111/jav.01341.

O'Connor, R.S., Wolf, B.O., Brigham, R.M., and McKechnie, A.E. 2017b. Avian thermoregulation in the heat: efficient evaporative cooling in two southern African nightjars. J. Comp. Physiol. B **187**(3): 477–491. doi:10.1007/s00360-016-1047-4.

Pattinson, N.B., and Smit, B. 2017. Seasonal behavioral responses of an arid-zone passerine in a hot environment. Physiol. Behav. **179**(June): 268–275. doi:10.1016/j.physbeh.2017.06.018.

Pincebourde, S., Murdock, C.C., Vickers, M., and Sears, M.W. 2016. Fine-scale microclimatic variation can shape the responses of organisms to global change in both natural and urban environments. Integr. Comp. Biol. **56**(1): 45–61. doi:10.1093/icb/icw016.

Porter, W.P., and Gates, D.M. 1969. Thermodynamic equilibria of animals with environment. Ecol. Monogr. **39**(3): 227–244.

Porter, W.P., Munger, J.C., Stewart, W.E., Budaraju, S., and Jaeger, J. 1994. Endotherm energetics - from a scalable individual-based model to ecological applications. Aust. J. Zool. **42**(1): 125. doi:10.1071/ZO9940125.

Porter, W.P., Ostrowski, S., and Williams, J.B. 2010. Modeling animal landscapes. Physiol. Biochem. Zool. **83**(5): 705–712. doi:10.1086/656181.

Potter, K.A., Woods, H.A., and Pincebourde, S. 2013. Microclimatic challenges in global change biology. Glob. Chang. Biol. **19**(10): 2932–2939. doi:10.1111/gcb.12257.

Scheffers, B.R., Edwards, D.P., Diesmos, A., Williams, S.E., and Evans, T.A. 2014.

496 Microhabitats reduce animal's exposure to climate extremes. Glob. Chang. Biol. **20**(2):
497 495–503. doi:10.1111/gcb.12439.
498 Schwenk, K., Padilla, D.K., Bakken, G.S., and Full, R.J. 2009. Grand challenges in organismal
499 biology. Integr. Comp. Biol. **49**(1): 7–14. doi:10.1093/icb/icp034.
500 Sears, M.W., and Angilletta, M.J. 2011. Introduction to the Symposium: responses of organisms
501 to climate change: a synthetic approach to the role of thermal adaptation. Integr. Comp.
502 Biol. **51**(5): 662–665. doi:10.1093/icb/icr113.
503 Sears, M.W., Raskin, E., and Angilletta, M.J. 2011. The world is not flat: defining relevant
504 thermal landscapes in the context of climate change. Integr. Comp. Biol. **51**(5): 666–675.
505 doi:10.1093/icb/icr111.
506 Smit, B., Harding, C.T., Hockey, P.A.R., and McKechnie, A.E. 2013. Adaptive thermoregulation
507 during summer in two populations of an arid-zone passerine. Ecology **94**(5): 1142–1154.
508 doi:10.1890/12-1511.1.
509 Smith, M.S., Horrocks, L., Harvey, A., and Hamilton, C. 2011. Rethinking adaptation for a 4 °C
510 world. Philos. Trans. R. Soc. A Math. Phys. Eng. Sci. **369**(1934): 196–216.
511 doi:10.1098/rsta.2010.0277.
512 Steyn, P. 1971. Notes on the breeding biology of the freckled nightjar. Ostrich **42**: 179–188.
513 doi:10.1080/00306525.1971.9633405.
514 Tieleman, B.I., van Noordwijk, H.J., and Williams, J.B. 2008. Nest site selection in a hot desert:
515 trade-off between microclimate and predation risk? Condor **110**(1): 116–124.
516 doi:10.1525/cond.2008.110.1.116.116.
517 Tieleman, B.I., and Williams, J.B. 1999. The role of hyperthermia in the water economy of
518 desert birds. Physiol. Biochem. Zool. **72**(1): 87–100. doi:10.1086/316640.

519 Tieleman, B.I., and Williams, J.B. 2002. Effects of food supplementation on behavioural
520 decisions of hoopoe-larks in the Arabian desert: balancing water, energy and
521 thermoregulation. Anim. Behav. **63**(3): 519–529. doi:10.1006/anbe.2001.1927.
522 Walsberg, G.E., and Weathers, W.W. 1986. A simple technique for estimating operative
523 environmental temperature. J. Therm. Biol. **11**(1): 67–72. doi:10.1016/0306-
524 4565(86)90020-3.
525 Walsberg, G.E., and Wolf, B.O. 1996. An appraisal of operative temperature mounts as tools for
526 studies of ecological energetics. Physiol. Zool. **69**(3): 658–681.
527 doi:10.1086/physzool.69.3.30164221.
528 Ward, D., and Pinshow, B. 1995. Temperature regulation of the great grey shrike (*Lanius*
529 *excubitor*) in the Negev desert—II. Field measurements of standard operative temperatures
530 and behaviour. J. Therm. Biol. **20**(3): 271–279. doi:10.1016/0306-4565(94)00051-J.
531 Watson, C.M., and Francis, G.R. 2015. Three dimensional printing as an effective method of
532 producing anatomically accurate models for studies in thermal ecology. J. Therm. Biol. **51**:
533 42–46. doi:10.1016/j.jtherbio.2015.03.004.
534 Weller, M. 1958. Observations on the incubation behavior of a common nighthawk. Auk **75**(1):
535 48–59.
536 Williams, J.B., Tieleman, B.I., and Shobrak, M. 1999. Lizard burrows provide thermal refugia
537 for larks in the Arabian desert. Condor **101**(3): 714–717. doi:10.2307/1370208.
538 Williams, S.E., Shoo, L.P., Isaac, J.L., Hoffmann, A.A., and Langham, G. 2008. Towards an
539 integrated framework for assessing the vulnerability of species to climate change. PLoS
540 Biol. **6**(12): e325. doi:10.1371/journal.pbio.0060325.
541 Wolf, B. 2000. Global warming and avian occupancy of hot deserts: a physiological and

behavioral perspective. Rev. Chil. Hist. Nat. **73**(3): 395–400. doi:10.4067/S0716-078X2000000300003.

Wolf, B.O., and Walsberg, G.E. 1996. Thermal effects of radiation and wind on a small bird and implications for microsite selection. Ecology **77**(7): 2228–2236. doi:10.2307/2265716.

Wolf, B.O., Wooden, K.M., and Walsberg, G.E. 1996. The use of thermal refugia by two small desert birds. Condor **98**(2): 424–428. doi:10.2307/1369162.

Woods, C.P., and Brigham, R.M. 2008. Common poorwill activity and calling behavior in relation to moonlight and predation. Wilson J. Ornithol. **120**(3): 505–512. doi:10.1676/06-067.1.

Woods, H.A., Dillon, M.E., and Pincebourde, S. 2015. The roles of microclimatic diversity and of behavior in mediating the responses of ectotherms to climate change. J. Therm. Biol. **54**: 86–97. doi:10.1016/j.jtherbio.2014.10.002.

555

556 **Table 1.** Mean ± SD diurnal (i.e., sunrise to sunset), midday (i.e., 12:00 – 15:00 hours) and
557 maximum operative temperatures (T_e ºC) recorded at six roost sites and one nest site used by six
558 different Rufous-cheeked Nightjars (*Caprimulgus rufigena*; roosts 1 and 2 were occupied by the
559 same individual). T_e was recorded at each site separately between 26 October and 12 December
560 2015, near Kimberly, South Africa at 1-minute intervals using two types of 3-D printed models,
561 including one type covered with skin and feathers (i.e., skin) and one without skin and feathers
562 (i.e., plastic). Sample sizes were identical between skin and plastic models, ranging from 2352 to
563 3497 for diurnal measurements and 543 to 806 for midday measurements. Values in parentheses
564 represent T_e ranges.

Site	Mean diurnal T_e		Mean midday T_e		Mean maximum T_e	
	Skin	Plastic	Skin	Plastic	Skin	Plastic
Roost 1	40.4 ± 11.4 (14.3 – 65.6)	40.6 ± 12.6 (16.6 – 64.8)	49.9 ± 7.6 (36.6 – 65.6)	50.3 ± 7.1 (39.1 – 64.8)	60.8 ± 6.0 (54.1 – 65.6)	62.8 ± 2.9 (59.5 – 64.8)
Roost 2	37.0 ± 6.7 (13.9 – 53.5)	41.0 ± 9.4 (14.0 – 62.0)	41.4 ± 3.1 (38.3 – 53.5)	41.4 ± 2.3 (37.2 – 52.4)	48.1 ± 5.5 (40.5 – 53.5)	58.3 ± 3.8 (53.0 – 62.0)
Roost 3	28.9 ± 6.2 (11.5 – 43.6)	29.2 ± 6.6 (10.9 – 44.7)	33.1 ± 3.3 (28.4 – 43.6)	33.0 ± 3.7 (28.0 – 44.7)	38.5 ± 4.6 (32.5 – 43.6)	38.9 ± 5.2 (32.7 – 44.7)
Roost 4	38.3 ± 10.3 (10.2 – 55.5)	37.8 ± 11.0 (8.3 – 55.5)	45.2 ± 3.6 (39.1 – 51.5)	45.3 ± 5.4 (35.9 – 53.4)	50.1 ± 4.8 (43.9 – 55.5	52.0 ± 5.5 (43.8 – 55.5)
Roost 5	31.0 ± 9.1 (6.6 – 48.7)	34.7 ± 10.8 (8.0 – 55.0)	36.5 ± 1.9 (31.5 – 42.1)	38.1 ± 4.4 (28.8 – 47.2)	43.0 ± 4.0 (39.9 – 48.7)	50.0 ± 6.3 (41.5 – 55.0)
Roost 6	41.3 ± 11.7 (16.9 – 62.6)	40.6 ± 12.1 (14.6 – 62.2)	44.5 ± 7.3 (33.8 – 60.3)	44.5 ± 7.3 (31.1 – 57.6)	58.2 ± 4.7 (53.2 – 62.6)	59.3 ± 2.7 (56.9 – 62.2)
Nest	41.0 ± 11.5 (15.4 – 60.4)	40.6 ± 11.2 (15.0 – 62.0)	51.4 ± 4.2 (44.5 – 60.4)	51.1 ± 4.9 (42.1 – 62.0)	55.1 ± 4.5 (49.5 – 60.4)	56.0 ± 4.9 (50.0 – 62.0)

565

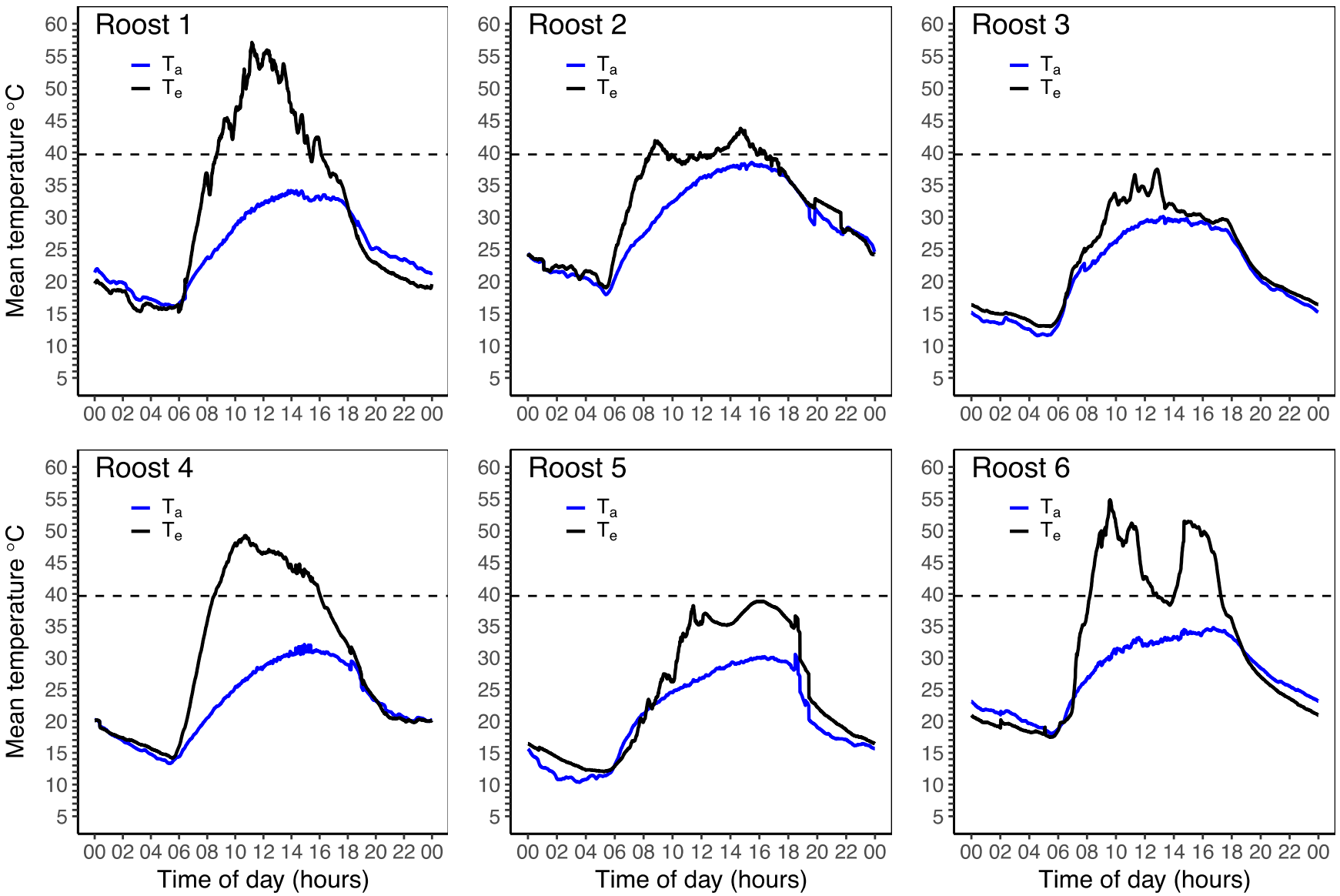
Roost 1
Roost 2
Roost 3
Roost 4
Roost 5
Roost 6
T_a
T_e
Mean temperature °C
Time of day (hours)
60 55 50 45 40 35 30 25 20 15 10 5
00 02 04 06 08 10 12 14 16 18 20 22 00

Figure 2. Mean operative temperature (T_e) and air temperature (T_a) for a 24-hour day (e.g., 02 = 02:00 hours; 22 = 22:00 hours) at six roost sites used by five Rufous-cheeked Nightjars (*Caprimulgus rufigena*; roosts 1 and 2 are from the same bird). T_e was recorded at 1-min intervals using a 3-D printed model covered with the skin and feathers of a Rufous-cheeked Nightjar. T_e was recorded at each roost site separately and remained at a site for approximately four days. Horizontal dashed lines represent free-ranging modal body temperature for roosting Rufous-cheeked Nightjars (39.7 ºC; O'Connor et al. 2017a). T_a was also recorded at 1-minute intervals.

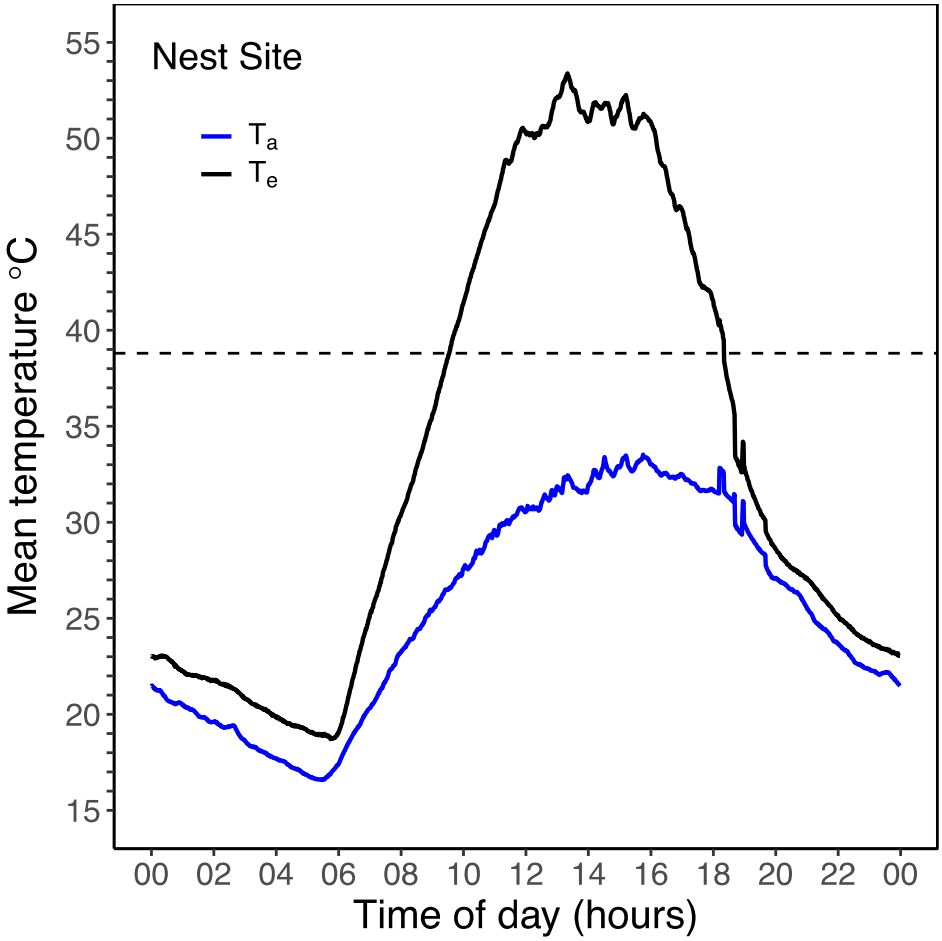

Figure 3. Mean operative temperature (T_e) and air temperature (T_a) for a 24-hour day (e.g., 02 = 02:00 hours; 22 = 22:00 hours) at a Rufous-cheeked Nightjar (*Caprimulgus rufigena*) nest site. T_e was recorded at 1-min intervals using a 3-D printed model covered with the skin and feathers of a Rufous-cheeked Nightjar. The model remained at the site for approximately four days. The horizontal dashed line represents the free-ranging modal body temperature for an incubating Rufous-cheeked Nightjar (38.8 ºC; O'Connor et al. 2017a). T_a was also recorded at 1-minute intervals.

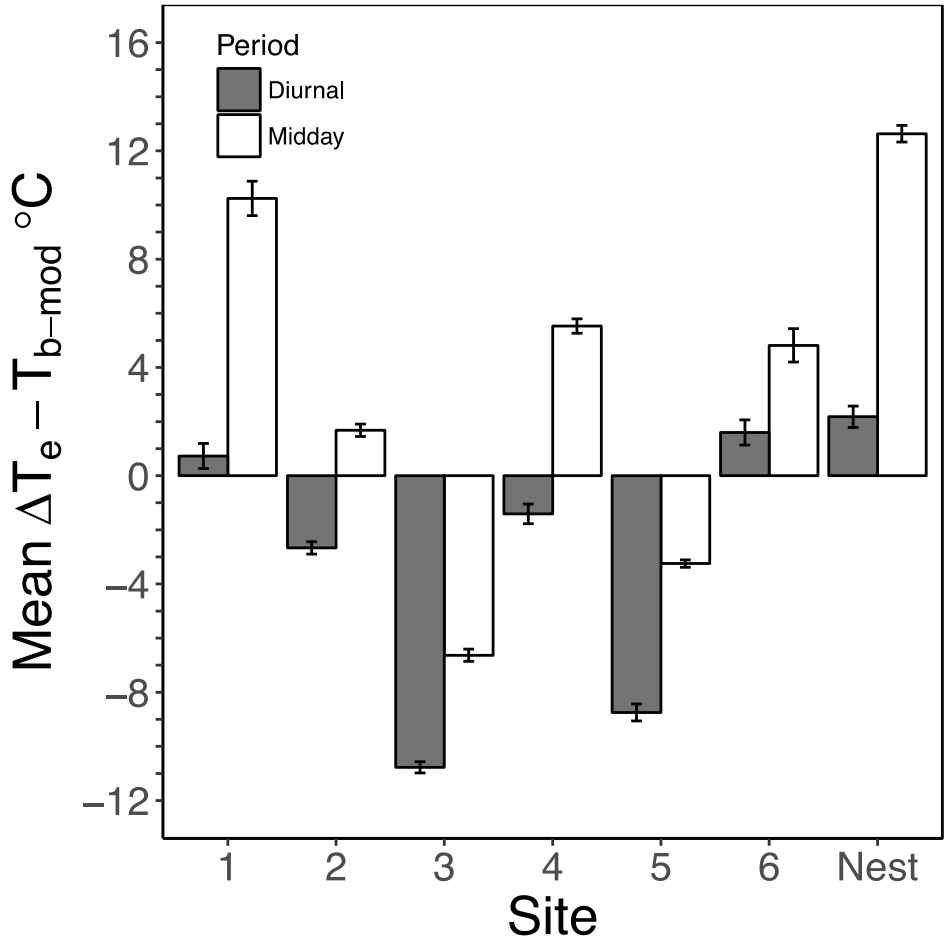

Figure 4. Mean difference between operative temperature (T_e) and free-ranging modal body temperature ($T_{b\text{-}mod}$) during the diurnal (i.e., sunrise to sunset) and midday (i.e., 12:00 – 15:00 hours) periods at six roost sites and one nest site used by six Rufous-cheeked Nightjars (*Caprimulgus rufigena*; roosts 1 and 2 are from the same individual). T_e was recorded at each site separately between 26 October and 12 December 2015, near Kimberly, South Africa at 1-minute intervals using a 3-D printed model covered with the skin and feathers of a Rufous-cheeked Nightjar. Error bars represent 95% confidence intervals.

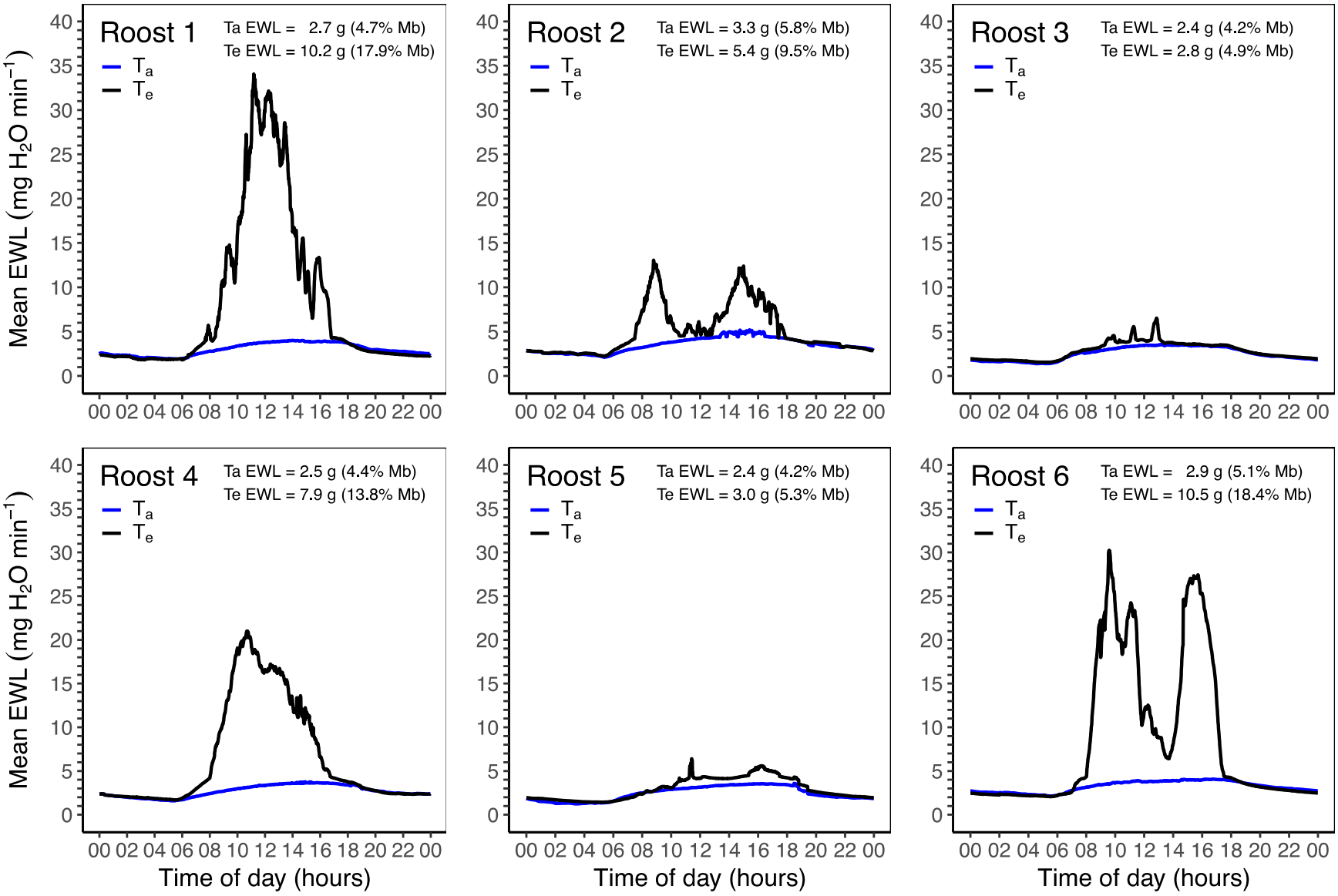
Roost 1
Ta EWL = 2.7 g (4.7% Mb)
Te EWL = 10.2 g (17.9% Mb)
Roost 2
Ta EWL = 3.3 g (5.8% Mb)
Te EWL = 5.4 g (9.5% Mb)
Roost 3
Ta EWL = 2.4 g (4.2% Mb)
Te EWL = 2.8 g (4.9% Mb)
Roost 4
Ta EWL = 2.5 g (4.4% Mb)
Te EWL = 7.9 g (13.8% Mb)
Roost 5
Ta EWL = 2.4 g (4.2% Mb)
Te EWL = 3.0 g (5.3% Mb)
Roost 6
Ta EWL = 2.9 g (5.1% Mb)
Te EWL = 10.5 g (18.4% Mb)
Ta
Te
Mean EWL (mg H2O min−1)
Time of day (hours)
00 02 04 06 08 10 12 14 16 18 20 22 00
0 5 10 15 20 25 30 35 40

Figure 5. Mean evaporative water loss (EWL) predictions for a 24-hour day (e.g., 02 = 02:00 hours; 22 = 22:00 hours) at six roost sites used by five Rufous-cheeked Nightjars (*Caprimulgus rufigena*; roosts 1 and 2 were used by the same bird). EWL was predicted every minute by plugging either T_e or T_a into EWL models from O'Connor et al. (2017b). Ta EWL and Te EWL represent the sum of all mean EWL predictions at each minute for only the diurnal period. Values in parentheses represent the amount of water lost during the diurnal period as a percentage of body mass (57.1 g).

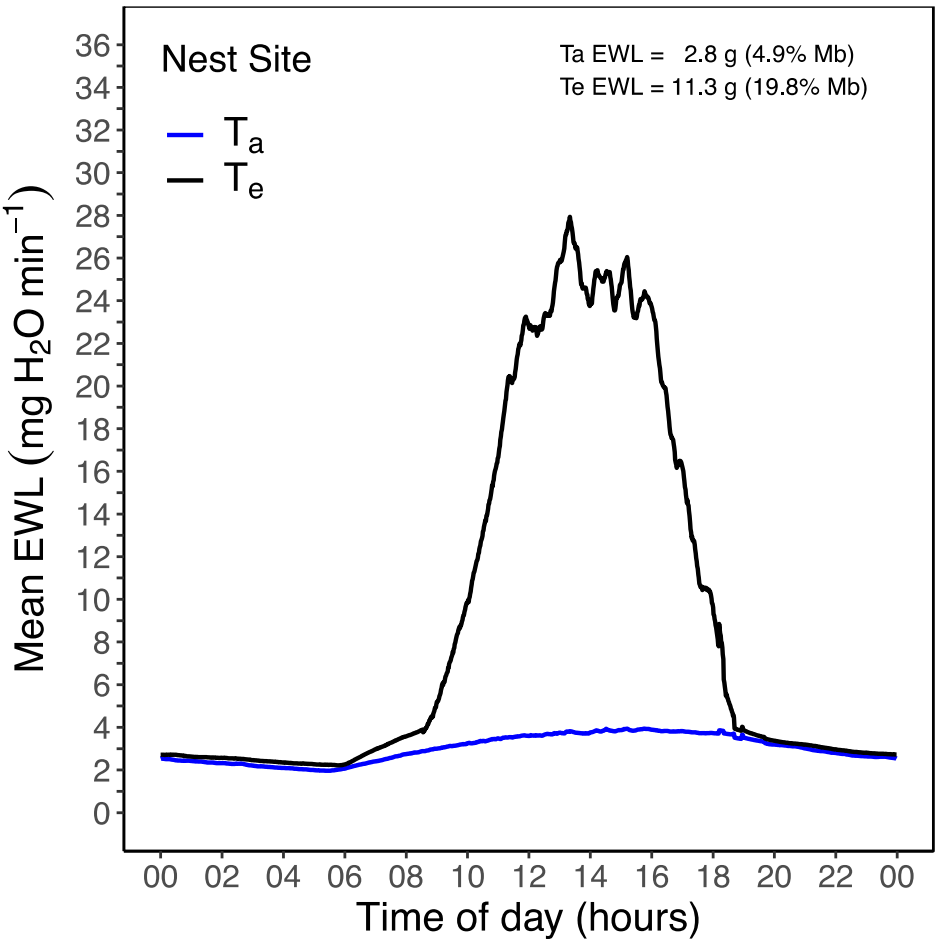

Figure 6. Mean evaporative water loss (EWL) predictions for a 24-hour day (e.g., 02 = 02:00 hours; 22 = 22:00 hours) for a Rufous-cheeked Nightjar (*Caprimulgus rufigena*) nest site. EWL was predicted every minute from T_e or T_a using EWL data from O'Connor et al. (2017b). Ta EWL and Te EWL represent the sum of all mean EWL predictions at each minute for only the diurnal period. Values in parentheses represent the amount of water lost during the diurnal period as a percentage of mean Rufous-cheeked Nightjar body mass (57.1 g).